Energy, exergy, and environmental analyses of renewable hydrogen production through plasma gasification of microalgal biomass

Kuo, Po Chih; Illathukandy, Biju; Wu, Wei; Chang, Jo Shu

DOI
10.1016/j.energy.2021.120025

Publication date
2021

Document Version
Final published version

Published in
Energy

Energy 223 (2021) 120025

Contents lists available at ScienceDirect

Energy

journal homepage: www.elsevier.com/locate/energy

Energy, exergy, and environmental analyses of renewable hydrogen production through plasma gasification of microalgal biomass

Po-Chih Kuo [a, *], Biju Illathukandy [b, c], Wei Wu [d], Jo-Shu Chang [d, e, f]

[a] Process and Energy Department, Faculty of 3mE, Delft University of Technology, Leeghwaterstraat 39, 2628, CB, Delft, the Netherlands
[b] Centre for Rural Development & Technology, Indian Institute of Technology, Delhi, 110016, India
[c] Department of Mechanical Engineering, Government Engineering College, Kozhikode, Kerala, 673005, India
[d] Department of Chemical Engineering, National Cheng Kung University, Tainan, 70101, Taiwan
[e] Department of Chemical and Materials Engineering, Tunghai University, Taichung, 407, Taiwan
[f] Research Center for Smart Sustainable Circular Economy, Tunghai University, Taichung, 407, Taiwan

ARTICLE INFO

Article history:
Received 12 November 2020
Received in revised form
25 January 2021
Accepted 31 January 2021
Available online 3 February 2021

Keywords:
Hydrogen production
Microalgal biomass
Plasma gasification
CO_2 emissions
3E analyses
Process simulation

ABSTRACT

In this study, an energy, exergy, and environmental (3E) analyses of a plasma-assisted hydrogen production process from microalgae is investigated. Four different microalgal biomass fuels, namely, raw microalgae (RM) and three torrefied microalgal fuels (TM200, TM250, and TM300), are used as the feedstock for steam plasma gasification to generate syngas and hydrogen. The effects of steam-to-biomass (S/B) ratio on the syngas and hydrogen yields, and energy and exergy efficiencies of plasma gasification ($\eta_{En,PG}$, $\eta_{Ex,PG}$) and hydrogen production (η_{En,H_2}, η_{Ex,H_2}) are taken into account. Results show that the optimal S/B ratios of RM, TM200, TM250, and TM300 are 0.354, 0.443, 0.593, and 0.760 respectively, occurring at the carbon boundary points (CBPs), where the maximum values of $\eta_{En,PG}$, $\eta_{Ex,PG}$, η_{En,H_2}, and η_{Ex,H_2} are also achieved. At CBPs, torrefied microalgae as feedstock lower the $\eta_{En,PG}$, $\eta_{Ex,PG}$, η_{En,H_2}, and η_{Ex,H_2} because of their improved calorific value after undergoing torrefaction, and the increased plasma energy demand compared to the RM. However, beyond CBPs the torrefied feedstock displays better performance. A comparative life cycle analysis indicates that TM300 exhibits the highest greenhouse gases (GHG) emissions and the lowest net energy ratio (NER), due to the indirect emissions associated with electricity consumption.

1. Introduction

The demand for clean energy from renewable and sustainable resources has been receiving much attention worldwide over the past decades, owing to the various environmental issues induced by the usage of fossil-based resources. Producing clean hydrogen from renewable resources is nowadays considered as one of the most important green energy technologies, due to its high energy content and potential applications in power, energy, chemical, and transportation sectors [1–3]. Converting biomass into hydrogen has thus been regarded as an alternative pathway to the fossil fuels such as natural gas and coal, as it promotes sustainable development. In this aspect, several hydrogen production technologies including thermochemical and biological conversions of lignocellulosic or algal biomass materials have actively been developed in the recent years [4–6]. Amongst all the known methods, biomass gasification is currently being used extensively to produce high purity hydrogen. This route generally involves the following major steps [3,7–9]: (1) hydrogen-rich syngas production through a biomass steam gasification (BSG); (2) high- and low-temperature water gas shift (WGS) reaction; and, finally, (3) hydrogen separation and purification as well as CO_2 capture by using a pressure swing adsorption (PSA) process.

However, one of the unfavorable issues raised during the biomass gasification is tar formation, a complex mixture of organic compounds which causes operational problems like blockage and corrosion in the process equipment or carbon deposition on the catalyst [10]. Compared to the conventional biomass gasification, plasma gasification is particularly advantageous to intensify tar cracking reaction with the high temperature plasma, thereby contributing to complete tar destruction, especially the heavy tar compounds [11,12]. Moreover, plasma-assisted biomass gasification

* Corresponding author.;
E-mail addresses: pckuo225@gmail.com, p.c.kuo@tudelft.nl (P.-C. Kuo).

https://doi.org/10.1016/j.energy.2021.120025

is beneficial to increase the reaction kinetics and gas productivity [13]. To explore the performance of plasma gasification of biomass, Hlina et al. [11] experimentally carried out the plasma gasification of wood sawdust (spruce) and wood pellets, and generated high-quality syngas with negligible tar content. Diaz et al. [14], based on the plasma gasification experiments of several types of biomass with steam, reported that the hydrogen concertation in product gas, and the plasma gasification efficiency (PGE) ranged from 52.4% vol. To 77.0% vol. And 24%–51%, respectively. Favas et al. [15] modeled the plasma gasification of forest residues, coffee husk, and vines pruning using a mixture of air and steam as gasifying agent in Aspen Plus. It was concluded that the amount of steam injected to the plasma gasifier had a profound effect on the hydrogen concentration in syngas. From all the above cited literature, it is evident that plasma-assisted gasification is a promising technology to enhance the syngas quality.

The utilization of algal biomass as an alternative feedstock to lignocellulosic biomass for syngas production through gasification has gained increasing interest primarily owing to its high productivity and photosynthetic efficiency, thereby having a great potential to reduce greenhouse gas (GHG) emissions via CO_2 biosequestration [4,16–18]. Many researchers have focused on both experimental and modelling studies of microalgae gasification. For example, López-González et al. [19] evaluated the performance of steam gasification at three different temperatures (850, 900, and 950 °C) from three species of microalgae (*Chlorella vulgaris, Scenedesmus almeriensis, and Nannochloropsis gaditana*) by using a thermogravimetric-mass spectrometric (TGA-MC) analysis. It was revealed that the mineral content in the microalgae deeply affected the gasification reactivity, and *Nannochloropsis gaditana* microalgae took the longest time to attain a char conversion of 100%. Duman et al. [20] investigated the catalytic steam gasification characteristics of three algal biomass materials (*Fucus serratus*, *Laminaria digitate*, and *Nannochloropsis oculate*) for hydrogen production in a two-stage fixed bed reactor. The *Fucus serratus* sample had the highest hydrogen yield with a tar conversion of 100%, whereas the tar conversion of *Nannochloropsis oculate* sample did not exceed 70% because of the high content of Na_2CO_3 in the microalgae. Adnan et al. [16] did a thermodynamic modelling to study the gasification performance of microalgae *(Spirulina)* with a mixture of steam and oxygen, and observed that the highest overall system efficiency was 52% at a steam-to-carbon (S/C) molar ratio of 1.0. Subsequently, Adnan et al. [17] also designed a microalgae (*Porphyra*) gasification system for the co-production of H_2-rich syngas and electricity. They outlined that higher moisture content in the microalgae had a negative impact on both overall system energy and exergy efficiencies.

In contrast to the widespread use of algal biomass to produce sustainable biofuels, torrefied algal biomass has also received a good deal of attention recently. This is ascribed to its multiple merits like higher carbon content and energy density, lower oxygen and moisture content (hydrophobicity), and greater grindability, compared to the raw microalgae [21–24]. The improvements of physical and chemical properties via torrefaction make algal biomass more appropriate and efficient to be applied for the multi-energy conversion systems. Yang et al. [25] examined the co-gasification of microalgal (*Spirulina platensis*) torrefied pellet and woody biomass (*Eucalyptus globulus*) torrefied pellet in a bubbling fluidized bed gasifier under the air environment. The maximum lower heating value (LHV) of the product gas was obtained with a blend of 30% microalgal torrefied pellet and 70% woody biomass torrefied pellet. Guo et al. [26] investigated the gasification characteristics of raw and torrefied macroalgae in a fixed reactor. It was highlighted that the latter one displayed the improved char reactivity at a gasification temperature of 1000 °C on account of the increased Na content and the decreased uniformity of the carbonaceous structure in the torrefied macroalgal char.

Based on the aforementioned review of relevant literature it is evident that a combination of torrefaction and gasification of algal biomass is a prospective approach to upgrade the quality of syngas. However, at present, there are no works that assessed the renewable hydrogen production from raw and torrefied microalgae using plasma gasification technology. Furthermore, to the best knowledge of the authors, the potential end-use applications of microalgae-derived syngas from plasma gasification and the environmental analysis of plasma-assisted microalgae-to-renewable hydrogen have also not yet been explored. As a result, the objectives of this work are: (1) to examine the performance of steam plasma gasification of four various microalgal biomass fuels. The optimal operating conditions for each microalgal fuel are outlined in terms of energy and exergy efficiencies. (see Sections 4.1 and 4.2); (2) the potential end-use applications of microalgae-derived syngas is explored in detail (see Section 4.3); and (3) the energy, exergy, and environmental (3E) analyses of an overall microalgae-based hydrogen production plant is evaluated to give comprehensive insights to the development of plasma-assisted microalgae-to-energy technologies (see Sections 4.4 and 4.5).

2. System modelling

A plasma-assisted hydrogen plant from microalgae is developed in Aspen Plus V 8.8 simulator as shown in Fig. 1. The entire hydrogen plant is divided into two subsystems: (1) a steam plasma gasification system and a hydrogen production unit, and (2) a separation and purification system. These are described comprehensively in the following sections, and the detailed operating conditions of the key units are tabulated in Table 1. The selected thermodynamic property model is Peng-Robinson Boston Mathias (PR-BM) equation of state [2,27]. Four kinds of microalgal biomass materials are used as the feedstock to produce hydrogen, and these are raw microalgae (RM) (*spirulina platensis*), torrefied microalgae at 200 °C (TM200), 250 °C (TM250), and 300 °C (TM300) with a residence time of 30 min. The proximate and elemental analysis of the four microalgal biomass are presented in Table 2 [22]. It can be seen that with increasing torrefaction severity, the extent of improvement in physical and chemical characteristics of microalgae becomes better. That is, the higher the torrefaction temperature, the lower the oxygen to carbon (O/C) and hydrogen to carbon (H/C) molar ratios in the microalgal biomass, thereby leading to a greater higher heating value (HHV). According to their properties,

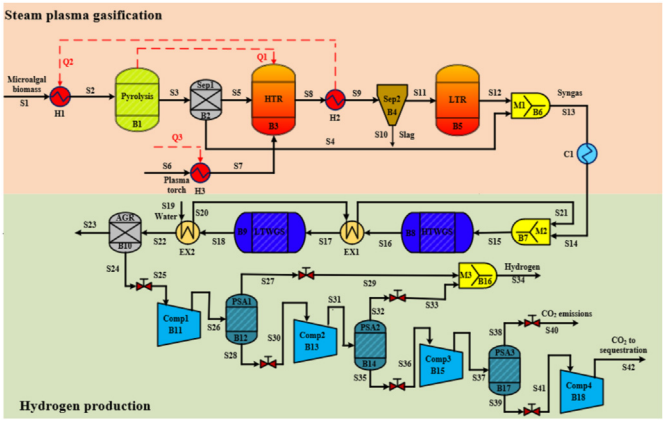

Fig. 1. Process flowsheet of a plasma-assisted hydrogen production plant from microalgae.

Table 1
Operating parameters used in the simulation.

Sub-systems	Parameters	Value	Reference
Plasma gasifier	Biomass inlet flow rate	100 kg h^{-1}	[49]
	S/B ratio	0.25–2	[15]
	Plasma gasifier temperature	2500 °C	[28]
	Plasma torch temperature	4000 °C	[28]
	Plasma torch efficiency	0.9	[29]
	Electrical efficiency of coal power plant	0.39	[33]
Water gas shift (WGS) reactor	High temperature reactor	400 °C	[32]
	Low temperature reactor	200 °C	[32]
Pressure swing adsorption (PSA)	Temperature	35 °C	[7]
	Pressure	30 atm	[7]
PSA-1	H_2 recovery (top stream)	95%	[7]
PSA-2	H_2 recovery (top stream)	95%	[7]
PSA-3	H_2 and CO_2 recovery (bottom stream)	0.5%/90%	[7]
CO_2 sequestration and storage	Temperature	30 °C	[8]
	Pressure	110 bar	[8]

Table 2
Proximate and elemental analysis of microalgal biomass used in the simulation [22].

Feedstocks	Raw microalgae (RM)	Torrefied microalgae at 200 °C (TM200)	Torrefied microalgae at 250 °C (TM250)	Torrefied microalgae at 300 °C (TM300)
Proximate analysis (wt% dry basis)				
Volatile matter	70.08	70.02	61.43	50.10
Fixed carbon	21.02	20.48	27.41	36.41
Ash	8.90	9.50	11.16	13.49
Elemental analysis (wt%, dry basis)				
C	45.69	47.95	53.07	58.46
H	7.71	6.74	6.40	6.30
N	11.26	11.04	11.89	11.82
O	25.69	23.82	16.83	9.47
S	0.75	0.95	0.65	0.46
HHV (MJ kg^{-1})	20.46	21.9	21.77	25.92
LHV (MJ kg^{-1})	18.58	20.39	20.32	24.51

four microalgal biomass fuels are set up in Aspen Plus as nonconventional components and the HCOALGEN and DCOALIGT models are selected to calculate their enthalpy and density [15,27].

2.1. Steam plasma gasification process

The process flowsheet of a steam plasma gasification system is shown in Fig. 1 (top part in pink background), where various unit operation blocks are connected in series to model the complex gasification phenomena in the plasma gasifier. An RYield reactor (B1) is used to model devolatilization of microalgae in the plasma gasifier in which the nonconventional microalgal biomass fuels (S2) are converted into conventional constituents (S3), i.e. H_2, O_2, N_2, S, solid carbon, and ash. The yields of each component are calculated in accordance with proximate and elemental analysis of various microalgal biomass fuels by performing FORTRAN codes (Table 2). After devolatilization, the conventional components are sent to a separator (B2) which simulates the evaporation of moisture contained in the microalgal biomass. A Sep block, which is a component separation operation by specifying the splits of each component, is used to model the evaporation of moisture in Aspen Plus simulation. The outlet stream of the separator is then fed to a high temperature RGibbs reactor (B3) which is operated at 2500 °C to model the major gasification reactions according to the chemical and phase equilibrium calculations by minimizing the Gibbs free energy [15,28]. On the other hand, a heater (H3) is used to simulate a DC non-transferred plasma torch to heat a plasma gas (steam) (S6) from 25 to 4000 °C (S7) [28,29]. The key gasification reactions occurring in the plasma gasifier are given below [12,27]:

Water gas reaction

$$C + H_2O \rightarrow CO + H_2, \quad \Delta H^0 = 131.4\ kJ\ mol^{-1} \tag{R1}$$

Water gas shift reaction

$$CO + H_2O \leftrightarrow CO_2 + H_2, \quad \Delta H^0 = -42\ kJ\ mol^{-1} \tag{R2}$$

Boudouard reaction

$$C + CO_2 \rightarrow 2\ CO, \quad \Delta H^0 = 172\ .6\ kJ\ mol^{-1} \tag{R3}$$

Methanation reaction

$$C + 2\ H_2 \leftrightarrow CH_4, \quad \Delta H^0 = -75\ kJ\ mol^{-1} \tag{R4}$$

Steam methane reforming

$$CH_4 + H_2O \leftrightarrow CO + 3H_2, \quad \Delta H^0 = 206\ kJ\ mol^{-1} \tag{R5}$$

An important operating parameter, steam-to-microalgal biomass (S/B) mass flow rate ratio in practicing steam plasma gasification of microalgae is defined as follows:

$$S/B = \frac{\dot{m}_{steam}}{\dot{m}_{microalgae}} \tag{1}$$

where $\dot{m}_{steam}$ and $\dot{m}_{microalgae}$ are the mass flow rate of the steam injected to the gasifier and microalgae (kg h^{-1}), respectively.

The outlet stream from the high temperature RGibbs reactor (S8) then passes through a separator (Sep block) (B4) to remove the residual slag (S10) and the rest (S11) is fed to a low temperature RGibbs reactor (B5) that is also modeled based on Gibbs free energy minimization approach at a temperature of around 1250 °C to complete the gasification reaction. The hot syngas (S13) from the

plasma gasifier is subsequently cooled down to 400 °C through a cooler (C1) and is sent to a hydrogen production, separation, and purification system.

The validation of the developed plasma gasifier model is carried out against the studies of Janajreh et al. [28] and Minutillo et al. [29]. Three materials, namely, refuse-derived fuel (RDF), municipal solid waste (MSW), and wood mentioned in the literature are chosen to be gasified with different plasma gas. The detailed operating conditions and validated results can be found in our previous study, where the simulated results using the developed model were in good agreement with those from the literature [30]. Furthermore, as shown in Table 3, the values of the root mean square error (RMSE) are very small for the three cases, meaning that the present model is thus reliable to accurately model the plasma gasification of microalgal biomass.

2.2. Hydrogen production, separation, and purification processes

The process flowsheet of hydrogen production and purification is shown in Fig. 1 (bottom part in green background), where it contains two water gas shift (WGS) reactors and a series of pressure swing adsorption (PSA) units. The obtained syngas (S14) from the plasma gasifier is first mixed with the required amount of pre-heated steam (S21) in a mixer (B7) and this mixture of gas then enters a high temperature sour water gas shift reaction (HTWGS) reactor (B8) with cobalt-molybdenum (CO/MO) based catalyst at 400 °C, followed by a low temperature WGS reactor (LTWGS) (B9) at 200 °C to produce H_2-rich gas [31,32]. Notably, in addition to WGS reaction (R2), COS in the product gas is simultaneously hydrolyzed into H_2S in the sour WGS reactor by R6 [31,32].

$$COS + H_2O \leftrightarrow H_2S + CO_2, \quad \Delta H^0 = -30.22\ kJ\ mol^{-1} \tag{R6}$$

The HT- and LT-WGS reactors are modeled using two adiabatic REquil reactor blocks for which chemical and phase equilibrium are calculated based on the reaction stoichiometry. On account of the exothermic WGS reaction, the heat generated from HTWGS and LTWGS reactors is recovered to generate steam through two heat exchangers (EX1 and EX2). A separator column (B10) is placed after the LTWGS reactor to remove the impurities H_2S, NH_3, and HCN in H_2-rich gas. Subsequently, the remaining H_2-rich gas is cooled down to 35 °C and compressed to 30 atm through a multi-stage compressor (B11) in order to achieve the inlet operating conditions of PSA [7]. Three PSA units (B12, B14, and B17) are adopted to simulate the hydrogen purification and CO_2 capture system and their detailed operating conditions are listed in Table 1 [7]. The hydrogen (S27) is thus separated by the PSA-1 unit (B12). Similarly, the off-gas from the PSA-1 unit (S28) is again compressed to 30 atm prior to entering the PSA-2 unit (B14). The produced H_2 from the PSA-1 and PSA-2 units is subsequently mixed in a mixer (B16) to form a high purity hydrogen product (99.99%), while the CO_2-rich gas (S35) leaving from the PSA-2 unit is compressed to 30 atm and fed to the PSA-3 unit (B17). The high concentration CO_2 (~98%) is finally captured and compressed to 110 bar (S42) for transportation and sequestration [8].

3. System performance analysis

In this study, the system performance of the proposed microalgae-to-renewable hydrogen energy plant is evaluated from the energy, exergy and environmental perspectives. Various performance indicators are described in detail below.

3.1. Energy analysis

Plasma energy to syngas production ratio (PSR) and plasma gasification energy efficiency ($\eta_{En,PG}$) are the two important indicators to address the energy performance of a plasma gasifier. They are expressed as follows:

$$\eta_{En,PG}\ (\%) = \frac{\dot{m}_{product\ gas} LHV_{product\ gas}}{\dot{m}_{microalgae} LHV_{microalgae} + E_{plasma}} \times 100\% \tag{2}$$

$$LHV_{product\ gas} = x_{H_2} LHV_{H_2} + x_{CO} LHV_{CO} + x_{CH_4} LHV_{CH_4} \tag{3}$$

$$PSR = \frac{E_{plasma}}{\dot{m}_{syngas}} \tag{4}$$

$$E_{plasma} = \frac{W_{torch}}{\eta_{torch} \times \eta_{electric}} \tag{5}$$

where $\dot{m}_{product\ gas}$ and $\dot{m}_{syngas}$ are the mass flowrate of product gas and syngas (kg s^{-1}) respectively. $LHV_{microalgae}$ and $LHV_{product\ gas}$ are the lower heating values of microalgae and product gas (MJ kg^{-1}) respectively, and $x_{H_2}, x_{CO}, x_{CH_4}$ are the mass fractions of H_2, CO, CH_4, respectively in the product gas. E_{plasma} is the plasma energy (MW), W_{torch} is the plasma torch power (MW), η_{torch} and $\eta_{electric}$ represent the plasma torch efficiency (90%) and electrical efficiency (39%), respectively [29,33].

For the overall system energy efficiency of a microalgae-based hydrogen production system, the hydrogen thermal energy efficiency (η_{En,H_2}) is defined as follows:

Table 3
Validation of the plasma gasifier model.

Feedstock	RDF		MSW		Wood	
Gas composition (vol. %)	Present model	Reference [29]	Present model	Reference [28]	Present model	Reference [28]
H_2	21.02	21.04	43.50	43.50	22.74	22.68
CO	33.79	33.79	34.40	34.50	36.43	36.45
CO_2	0	0	0.05	0.03	0.64	0.65
CH_4	5.99	5.97	0.01	0.01	0	0
H_2O	11.69	11.68	16.27	16.22	5.30	5.31
N_2	26.96	26.97	5.69	5.63	34.89	34.90
H_2S	0.22	0.22	0.08	0.09	0	0
COS	0.02	0.02	0	0	0	0
HCl	0.32	0.32	0	0	0	0
Torch power (MW)	4.25	4.26	4.07	4.06	7.85	7.84
RMSE[a]	0.01		0.04		0.02	

$$\eta_{En,H_2}\ (\%) = \frac{\dot{m}_{H_2} LHV_{H_2}}{\dot{m}_{microalgae} LHV_{microalgae} + E_{plasma} + W_{PSA}} \times 100\% \quad (6)$$

where $\dot{m}_{H_2}$ is the mass flowrate of hydrogen production rate (kg s^{-1}) and W_{PSA} is the total power consumption of the entire hydrogen purification process (MW).

3.2. Exergy analysis

The total exergy of material flow consists of physical exergy and chemical exergy, which can be expressed as follows [34]:

$$\dot{E}x_{total} = \dot{E}x_{ph} + \dot{E}x_{ch} \quad (7)$$

where $\dot{E}x_{total}$ is the total exergy of material flow (MW). $\dot{E}x_{ph}$ and $\dot{E}x_{ch}$ represent the physical and chemical exergy of the material flow (MW), respectively.

The physical exergy ($\dot{E}x_{ph}$) for each component in the product gas can be written as [34,35].

$$\dot{E}x_{ph} = \left(h - h_0\right) - T_0\left(s - s_0\right) \quad (8)$$

where h and s are the specific enthalpy (kJ $kmol^{-1}$) and entropy (kJ $kmol^{-1}$ K^{-1}) of the gas components at a given state, respectively. h_0 and s_0 are the specific enthalpy (kJ $kmol^{-1}$) and entropy (kJ $kmol^{-1}$ K^{-1})of the gas components at reference conditions ($T_0 = 25$ °C and $P_0 = 1$ at m), respectively.

The chemical exergy ($\dot{E}x_{ch}$) for each component in the gas mixture can be defined as follows [34,35]:

$$\dot{E}x_{ch} = \sum_i \dot{n}_i \left(Ex_{ch,i} + RT_0 \ln \frac{\dot{n}_i}{\sum \dot{n}_i}\right) \quad (9)$$

where $\dot{n}_i$ is the mole flow rate of component i in the gas mixture (kmol s^{-1}), $Ex_{ch,i}$ is the standard chemical exergy of component i in the gas mixture [35], and R is the gas constant (kJ $kmol^{-1}$ K^{-1}).

The chemical exergy of microalgae ($\dot{E}x_{microalgae}$) can be calculated by Refs. [34,35].

$$\dot{E}x_{microalgae} = \beta\ \ \dot{m}_{microalgae}\ \ LHV_{microalgae} \quad (10)$$

$$\beta = \frac{1.0412 + 0.2160H/C - 0.2499O/C(1 + 0.7884H/C) + 0.0450N/C}{1 - 0.3035O/C} \quad (O/C\ \leq 2.67) \quad (11)$$

where C, H, O, and N are the mass fractions of carbon, hydrogen, oxygen, and nitrogen in the microalgal biomass, respectively.

The plasma gasification exergy efficiency ($\eta_{Ex,PG}$) and hydrogen thermal exergy efficiency (η_{Ex,H_2}) are written as follows:

$$\eta_{Ex,PG}\ (\%) = \frac{\dot{m}_{product\ gas} Ex_{product\ gas}}{\dot{m}_{microalgae} Ex_{microalgae} + E_{plasma}} \times 100\% \quad (12)$$

$$\eta_{Ex,H_2}\ (\%) = \frac{\dot{m}_{H_2} Ex_{H_2}}{\dot{m}_{microalgae} Ex_{microalgae} + E_{plasma} + W_{PSA}} \times 100\% \quad (13)$$

where $Ex_{product\ gas}$, Ex_{H_2}, and $Ex_{microalgae}$ are the exergy rates of the product gas, hydrogen, and microalgae (MW), respectively.

3.3. Environmental analysis

A life cycle analysis (LCA) of microalgae-based hydrogen production process is performed according to the International Organization for Standardization (ISO) guidelines (14,040), in which there are four phases: goal and scope definition, life cycle inventory (LCI) analysis, life cycle impact assessment (LCIA), and life cycle interpretation. The major goal of this LCA is to quantify and compare the potential impacts that the four microalgal fuels (i.e. RM, TM200, TM250, and TM300) have on the environmental performance in terms of global warming potential (GWP) and net energy ratio (NER). The LCA boundary shown in Fig. 2 comprises of five main sub-sections: microalgae cultivation and harvest, drying, torrefaction, plasma gasification, and hydrogen production and purification. The GHG emissions and energy usage from the production of materials and infrastructure construction are, however, not included in the LCA calculation [36]. The functional unit of the LCA is to produce 1 kg of hydrogen using four various microalgae-based feedstocks. GHG emissions are the only impact category taken into account in this study. Three major GHG emissions namely CO_2, CH_4, and N_2O are considered to contribute directly to the GWP for a time horizon of 100 years, resulting in a GWP conversion factor of 1 for CO_2, 25 for CH_4, and 298 for N_2O to account for the net CO_2 equivalent (CO_2eq) emissions from the system boundary [37]. The net GHG emissions from the system boundary are thus expressed by

$$\begin{aligned} Net\ GHG\ emissions\ (kg\ CO_{2eq}) = &\sum CO_{2eq}\ direct\ emissions \\ &+ \sum CO_{2eq}\ indirect\ emissions \\ &- \sum CO_2\ fixation \end{aligned} \quad (14)$$

The life cycle NER is another vital indicator to account for the energetic effectiveness of the overall microalgae-based hydrogen production system and it is defined as the ratio of total useful energy produced from the system boundary divided by total primary fossil energy consumption due to production of 1 kg of hydrogen [38].

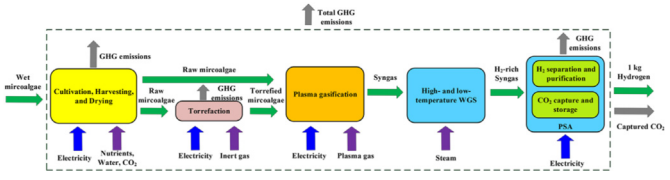

Fig. 2. LCA system boundary of a plasma-assisted hydrogen production plant from microalgae.

$$NER = \frac{Energy\ \ output\ \ (kWh)}{Energy\ \ input\ \ (kWh)} \quad (15)$$

The life cycle inventory (LCI) data of GHG emissions and energy usage from cultivation and harvest for producing 1 kg of wet microalgae (*Spirulina platensis*) is obtained from the studies of Collet et al. [39] and Campbell et al. [40]. The LCI data of drying process is provided by the study of Papadaki et al. [41], where it was reported that the energy consumption during the drying process of 8 kg of wet microalgae (88% moisture) to generate 1 kg of dry microalgae (<4% moisture) is 34.704 MJ. On the other hand, the mass loss during the torrefaction of dry microalgae is also necessary to be considered in the LCA calculation. According to the study of Wu et al. [22], the solid mass yield of torrefied microalgae is 90%, 76.26%, and 61.96% after undergoing torrefaction at 200 °C, 250 °C, and 300 °C, respectively. The LCI data of the torrefaction process at three various torrefaction temperatures of 200 °C, 250 °C, and 300 °C is estimated by applying the kinetic model of gas formation during torrefaction of microalgae provided by the study of Dhanavath et al. [42], while that of steam plasma gasification of microalgae and hydrogen production and purification are acquired from the results of Aspen Plus simulation. The overall LCI data for the microalgae-based hydrogen production process are listed in Table 4.

4. Results and discussion

In the following discussion, the plasma gasification characteristics of four microalgal biomass materials (i.e. RM, TM200, TM250, and TM300) are first investigated. The effort is made to find the optimal operating conditions (steam-to-biomass ratio) of the plasma gasifier to produce microalgal syngas and to assess its end-use applications. Subsequently, particular attention is paid to study the performance of the hydrogen production process using microalgae-derived syngas and examine the impacts of the four algal-based fuels on the overall system performance in terms of hydrogen yield, hydrogen energy (η_{En,H_2}) and exergy (η_{Ex,H_2}) efficiencies. An environmental analysis of the microalgal hydrogen production process is finally explored.

4.1. Syngas characteristics and optimization

The distributions of gas production rates of the four types of microalgal biomass materials as a function of S/B ratio are shown in Fig. 3, where the main components from the plasma gasifier are H_2 (Fig. 3a), CO (Fig. 3b), CO_2 (Fig. 3c), CH_4 (Fig. 3d), and unconverted char (Fig. 3e). It can be clearly seen that the H_2 production rate is highly dependent on the S/B ratio, no matter what fuel is tested (Fig. 3a). As a whole, the higher the S/B ratio, the higher the amount

Table 4
Life cycle inventory for the renewable hydrogen production from microalgal biomass.

Inventory	Inputs	Outputs	Source
Cultivation and harvest			[39,40]
1 kg of wet microalgae production at an open pond			
Carbon dioxide (kg)	1.4286	0.0193	
Energy (MJ)	1.3094		
Drying			[41]
1 kg of dry microalgae production			
Wet microalgae (kg)	8	–	
Energy (MJ)	34.704	–	
Torrefaction (1 kg of dry microalgae)			[42]
TM200			
Carbon dioxide (kg)	–	0.0474	
Methane (kg)	–	0	
Electricity (kWh)	0.0063		
TM250			
Carbon dioxide (kg)	–	0.0412	
Methane (kg)	–	0.0008	
Electricity (kWh)	0.0081	–	
TM300			
Carbon dioxide (kg)	–	0.1157	
Methane (kg)	–	0.0041	
Electricity (kwh)	0.0099	–	
Hydrogen production (1 kg of dry microalgae)			Aspen Plus results
RM			
Carbon dioxide (kg)	–	0.1382	
Hydrogen (kg)	–	0.1812	
Plasma electricity (kWh)	3.7080	–	
Hydrogen purification electricity (kWh)	1.1669	–	
TM200			
Carbon dioxide (kg)	–	0.1549	
Hydrogen (kg)	–	0.1937	
Plasma electricity (kWh)	4.6356	–	
Hydrogen purification electricity (kWh)	1.2739	–	
TM250			
Carbon dioxide (kg)	–	0.2152	
Hydrogen (kg)	–	0.1707	
Plasma electricity (kWh)	6.212	–	
Hydrogen purification electricity (kWh)	1.4076	–	
TM300			
Carbon dioxide (kg)	–	0.1893	
Hydrogen (kg)	–	0.2426	
Plasma electricity (kWh)	7.9583	–	
Hydrogen purification electricity (kWh)	1.5653	–	

Note: The emissions factor contributed by the electricity is estimated by 0.655 kg CO_{2eq} kWh^{-1} [50].

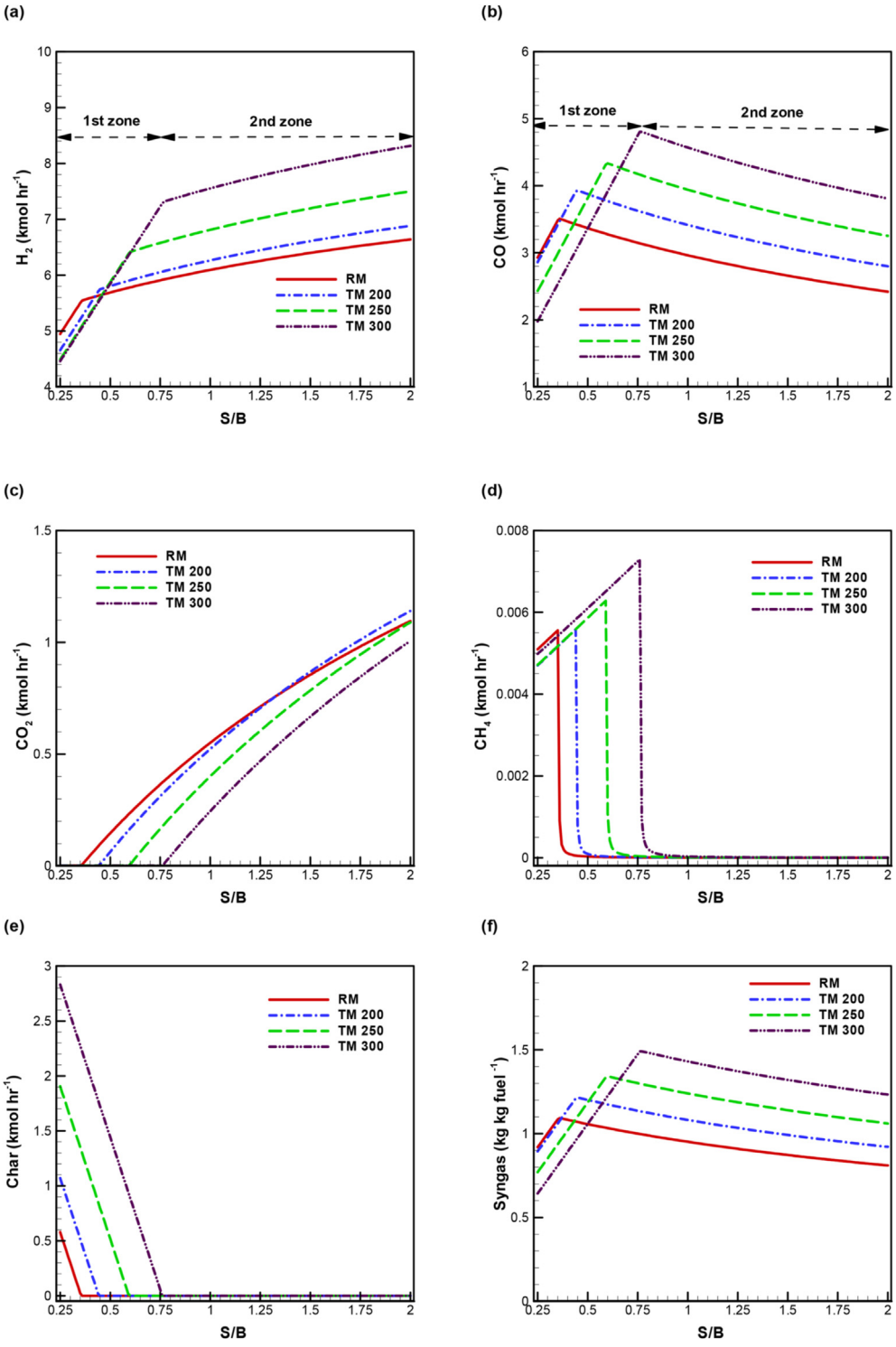

Fig. 3. Effect of the S/B ratio on the product flow rate and syngas yield from steam plasma gasification of four microalgal biomass fuels.

of H_2 generated. The H_2 production rate ranges from 4.95 to 6.64 kmol h^{-1} for RM, 4.66–6.88 kmol h^{-1} for TM200, 4.49–7.51 kmol h^{-1} for TM250, and 4.46–8.31 kmol h^{-1} for TM300, within the investigated range of S/B ratio. The dominant chemical reactions in the plasma gasifier for H_2 production are mainly endothermic water gas reaction (R1) and exothermic water gas shift reaction (R2). Also, it is noteworthy that the distribution of H_2 production rate of each microalgal fuel can be approximately partitioned into two reaction zones (TM300 is taken as an example in Fig. 3a). The first zone is primarily governed by R1, while the second one is majorly triggered by R2. This can also be explained by observing the distributions of CO production rate as shown in Fig. 3b, where the increasing and decreasing trends of CO production rate are observed. At lower S/B ratios, CO production rate is contributed by R1 (first zone). However, at higher S/B ratios, the carbon content in microalgae is completely reacted with steam,

thereby leading a significant decrease in CO production rate and a corresponding increase in CO_2 production rate (Fig. 3c) as a result of R2 (second zone). The highest CO production rate is approximately 3.51 kmol h^{-1} for RM, 3.93 kmol h^{-1} for TM200, 4.33 kmol h^{-1} for TM250, and 4.80 kmol h^{-1} for TM300.

The CH_4 production rate from steam plasma gasification of microalgae is relatively small, and its highest value is around 0.0056 kmol h^{-1} for both RM and TM200, 0.0063 kmol h^{-1} for TM250, and 0.0073 kmol h^{-1} for TM300. The CH_4 production is mainly attributed to the methanation reaction (R4). However, once the carbon in the microalgal biomass fuels is completely reacted, the produced CH_4 is further consumed by steam due to the steam methane reforming reaction (R5). This is also the reason why a maximum distribution is observed in Fig. 3d. The distributions of unconverted char are shown in Fig. 3e. It is observed that the carbon content in microalgal biomass material increases linearly with a rise in torrefaction temperature (Table 2) [22]. Consequently, as expected, higher amount of steam is required at elevated torrefaction temperatures to convert the total carbon contained in microalgal biomass fuel into syngas. On the other hand, it is worth noting that the second reaction zone of both H_2 and CO production rates (Fig. 3a and b) take place at distinct S/B ratios for each feedstock. In the studies of Prins et al. [34] and Kuo and Wu [43], the optimum energy and exergy efficiencies of the gasification system were achieved at the so-called carbon boundary point (CBP) at which the total char is completely reacted. To find the CBPs of each microalgal biomass fuel, the following constrained optimization algorithm with the objective of maximizing the syngas yield are implemented and solved in Aspen Plus according to the sequential quadratic programming (SQP) method:

$$\max_{u_{ij}} J_i = \dot{m}^{out}_{syngas}|_i = \frac{\dot{m}^{out}_{H_2} + \dot{m}^{out}_{CO}}{\dot{m}^{in}_{biomass}},\ i \in \text{microalgal biomass}\ (I, II, III, IV) \tag{16}$$

subject to

$$a_j \le u_{ij} \le b_j\ j = 1, 2 \tag{17}$$

$$0.25 \le S/B \triangleq \frac{\dot{m}_{steam}}{\dot{m}_{biomass}} \le 2 \tag{18}$$

where $\dot{m}^{out}_{syngas}|_i$ (kg kg-fuel^{-1}) is the objective function (J_i), I, II, III, IV are the four types of microalgal biomass materials, a_j and b_j represent the lower and upper bounds of u_{ij}, and $u_{ij} = [\dot{m}_{biomass}, \dot{m}_{steam}]^T_j$ is the steady-state operating condition.

Based on the specific optimization algorithm, the CBPs are obtained and located at S/B ratios of 0.354, 0.443, 0.593, and 0.760, corresponding to RM, TM200, TM250, and TM300, respectively, at which the maximum syngas yields of RM, TM200, TM250, and TM300 from the steam plasma gasification are 1.09, 1.22, 1.34, and 1.49 kg kg-fuel^{-1}, respectively, as shown in Fig. 3e. This reveals that the syngas yield of RM is amplified by 11.92%, 22.94%, and 36.70% for torrefied microalgae at 200 °C, 250 °C, and 300 °C respectively.

4.2. Plasma gasification efficiency

The distributions of the plasma energy to syngas production ratio (PSR), LHV of the product gas, and plasma gasification energy ($\eta_{En,PG}$) and exergy ($\eta_{Ex,PG}$) efficiencies of the four microalgal fuels with respect to the S/B ratios are plotted in Fig. 4. As shown in Fig. 4a, the values of PSR of RM, TM200, TM250, and TM300 range between 2.85 and 25.84 kWh kg^{-1}, 2.93–22.72 kWh kg^{-1}, 3.40–19.73 kWh kg^{-1}, and 4.07–16.98 kWh kg^{-1}, respectively, within the investigated range of S/B ratio. It should be noted from the results that the value of PSR for TM300 is the highest, followed by TM250 and TM200 at lower S/B ratios, whereas that of TM300 is the lowest when the S/B ratio is larger than around 0.7. This change is mainly due to a significant enhancement of syngas yield after torrefaction pretreatment of microalgae (Fig. 3f). As far as the LHV of the product gas from the plasma gasifier is concerned, Fig. 4b displays that the higher the S/B ratio, the lower the LHV of the product gas as a consequence of less combustible gases produced with the increase in S/B ratio. Similar trends are also observed in the study of Favas et al. [15] where forest residues, coffee husk, and vines pruning were gasified with steam in the plasma gasifier. As a whole, the values of LHV of the product gas are in the range of 7.85–18.49 MJ kg^{-1}, 8.45–18.88 MJ kg^{-1}, 9.46–19.51 MJ kg^{-1}, and 10.78–21.16 MJ kg^{-1}, corresponding to RM, TM200, TM250, and TM300, respectively. This implies that torrefaction of microalgae prior to the steam plasma gasification is conducive to improving the energy contents of the product gas, especially at higher torrefaction temperatures.

In the examination of the profiles of $\eta_{En,PG}$ and $\eta_{Ex,PG}$ as a function of S/B ratio, it can be seen in Fig. 4c and d that with the increase in S/B ratio, the trends of $\eta_{En,PG}$ and $\eta_{Ex,PG}$ of the four microalgal fuels first increase until they reach a maximum value which is exactly located at the CBPs and then decrease rapidly. Under the condition of CBP, the maximum values of ($\eta_{En,PG}$, $\eta_{Ex,PG}$) of RM, TM200, TM250, and TM300 are (73.10%, 66.39%) at S/B = 0.354, (67.49%, 61.87%) at S/B = 0.443, (65.09%, 60.06%) at S/B = 0.593, and (58.86%, 54.88%) at S/B = 0.760, respectively. Notably, although using torrefied microalgae as a feedstock for steam plasma gasification displays the decreased values of PSR (Fig. 4a) and the increased LHV of the product gas (Fig. 4b), the maximum value (obtained under the CBPs) of $\eta_{En,PG}$ (Fig. 4c) for TM200, TM250, and TM300 is reduced by 5.61%, 8.01%, 14.24% as compared to RM. This can be elucidated by the increased value of LHV of the torrefied microalgae, and the surge in plasma energy demand compared to the RM. For instance, the values of LHV of TM200, TM250, and TM300 are enhanced by a factor of 9.73%, 9.38%, and 31.92% when RM is torrefied at 200 °C, 250 °C, and 300 °C, respectively (Table 2). Nevertheless, if the S/B ratio of TM200, TM250, and TM300 is larger than 0.43, 0.48, and 0.60, respectively, the values of $\eta_{En,PG}$ can be increased by factors of 0.44–5.24%, 0.27–17.24%, and 0.05–26.87%, respectively, while those of $\eta_{Ex,PG}$ can be enhanced by factors of 0.86–5.30%, 0.61–17.15%, and 0.86–26.89%, respectively, compared to those of RM. The product gas rate, syngas yield, LHV of the product gas, PSR, $\eta_{En,PG}$, and $\eta_{Ex,PG}$ of four different microalgal fuels under the condition of CBP are summarized in Table 5. It is noteworthy that the total amount of *S*-containing compounds is reduced by 7.64% and 34.26%, whereas those of N-containing compounds are increased by 13.94% and 21.72%, when RM is torrefied at 250 °C and 300 °C, respectively. Their decrease and increase might be attributed to the lower sulfur and the higher nitrogen contents in TM250 and TM300 in comparison with RM (Table 2) [44].

4.3. Syngas end-use applications

Typically, biomass-derived syngas can be used in various applications as follows: (1) it can be converted to a wide range of liquid chemicals via the Fischer-Tropsch (FT) technology based on the specific H_2/CO molar ratio of the syngas (i.e. H_2/CO = 1, 2, and 3) [45]; (2) it can be combusted to generate heat and power in various combustion systems such as a gas turbine combined cycle or an internal combustion engine [46]; and (3) it can be utilized as an efficient fuel for solid oxide fuel cells (SOFCs) [47]. The results based

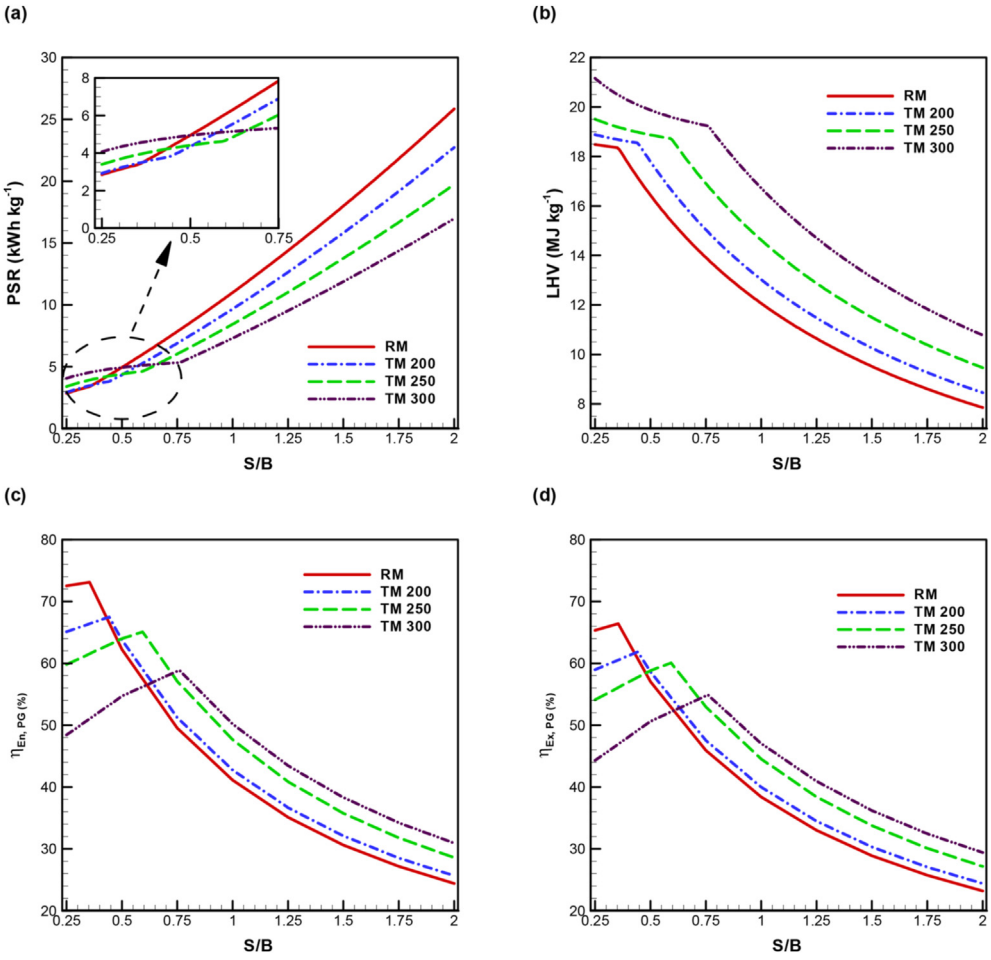

Fig. 4. Effect of the S/B ratio on the (a) plasma energy to syngas production ratio (PSR), (b) LHV of the product gas, (c) plasma gasification energy efficiency ($\eta_{En,PG}$), and (d) plasma gasification exergy efficiency ($\eta_{Ex,PG}$) of four microalgal biomass fuels.

Table 5
Plasma gasification performances of various microalgal fuels under the condition of CBP.

Feedstock	RM	TM200	TM250	TM300
S/B ratio at the CBP	0.354	0.443	0.593	0.760
Gas mass flowrate (kg hr^{-1})				
H_2	11.14	11.54	12.88	14.69
CO	98.21	110.10	121.40	134.60
CO_2	0.042	0.050	0.054	0.060
CH_4	0.089	0.090	0.10	0.12
H_2O	6.54	1.19	1.52	0.99
N_2	10.38	10.88	11.67	11.67
NH_3	0.0008	0.0009	0.0009	0.0010
HCN	0.036	0.037	0.041	0.044
H_2S	0.72	0.97	0.66	0.47
COS	0.036	0.052	0.035	0.024
H_2/CO (mol mol^{-1})	1.59	1.47	1.49	1.53
LHV (MJ kg^{-1})	18.35	18.55	18.73	19.23
Syngas yield (kg kg-$fuel^{-1}$)	1.09	1.22	1.34	1.49
PSR (kWh kg^{-1})	3.39	3.82	4.63	5.34
$\eta_{En,PG}$ (%)	73.10	67.49	65.09	58.86
$\eta_{Ex,PG}$ (%)	66.39	61.87	60.06	54.88

on the sensitivity analysis of S/B ratio (Fig. 3) demonstrate that plasma gasification of microalgae with steam is not a suitable route for the production of aldehydes (H_2/CO ratio = 1) and ammonia (H_2/CO ratio = 3) within the investigated range of S/B ratio, regardless of the microalgal feedstock examined. On the contrary,

Table 6
Operating conditions and performances of the steam plasma gasification for achieving a H_2/CO ratio of 2.

Feedstock	S/B ratio	$\eta_{En,PG}$ (%)	$\eta_{Ex,PG}$ (%)
RM	0.93	43.17	40.25
TM200	1.27	36.26	34.12
TM250	1.46	36.49	34.42
TM300	0.34	51.05	46.92
	1.65	35.75	33.86

the syngas with a H_2/CO ratio of 2, which can be directly utilized to produce FT liquids, is achievable for all types of microalgal fuels. The corresponding operating conditions of S/B ratio for achieving desired syngas quality are tabulated in Table 6.

With attention paid to the use of microalgal biomass-derived syngas for SOFCs, Fig. 5 shows a ternary C–H–O diagram, where the syngas composition produced from four types of microalgal fuels under the condition of CBP are plotted. Basically, the C–H–O diagram is helpful for preliminarily identifying the thermodynamic constraints on the solid carbon formation at given operating pressure and temperature when using syngas as fuel for SOFCs [47]. It is clear from Fig. 5 that the syngas composition of all types of torrefied microalgae lies above the carbon boundary line, no matter what operating temperature of SOFCs is examined, meaning that carbon deposition is possible to occur on SOFC anodes. It implies, in turn, that steam addition to TM-derived syngas is required to avoid

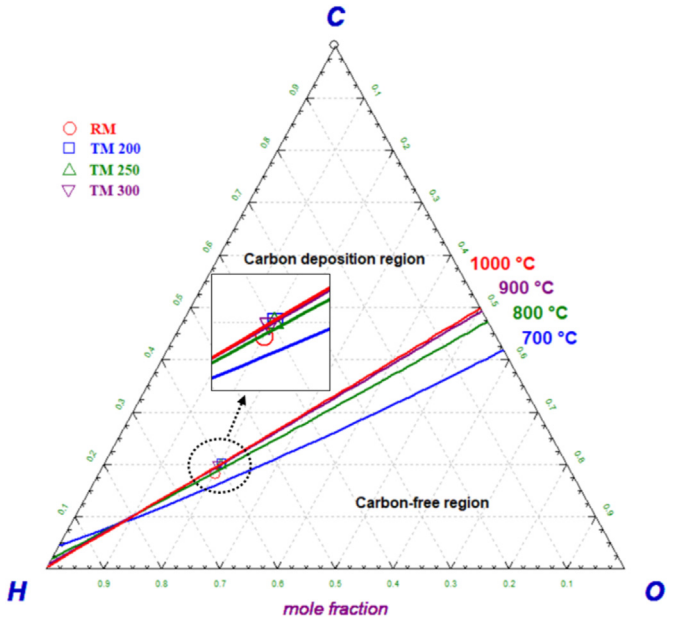

Fig. 5. C–H–O diagram for various SOFC operating temperatures of four microalgal biomass derived syngas.

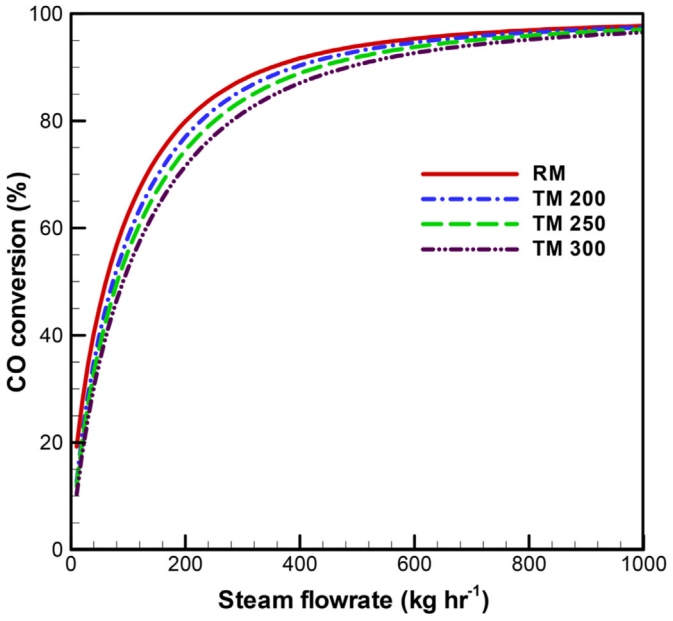

Fig. 6. Effects of the steam flowrate on the CO conversion in the high-temperature water gas shift (HT-WGS) reactor of four microalgal biomass derived syngas.

the risk of carbon formation [47]. In contrast, RM-derived syngas might be safe while considering the SOFC temperatures at 900 °C and 1000 °C.

4.4. Hydrogen production and overall system efficiency

In order to achieve a highly efficient hydrogen production system, the steam requirement for the water gas shift (WGS) reactor is a key parameter that influences the overall system energy efficiency [31]. The CO conversion as a function of the amount of steam injected into the HT-WGS reactor is shown in Fig. 6, where the syngas composition of each microalgal fuel is obtained under the

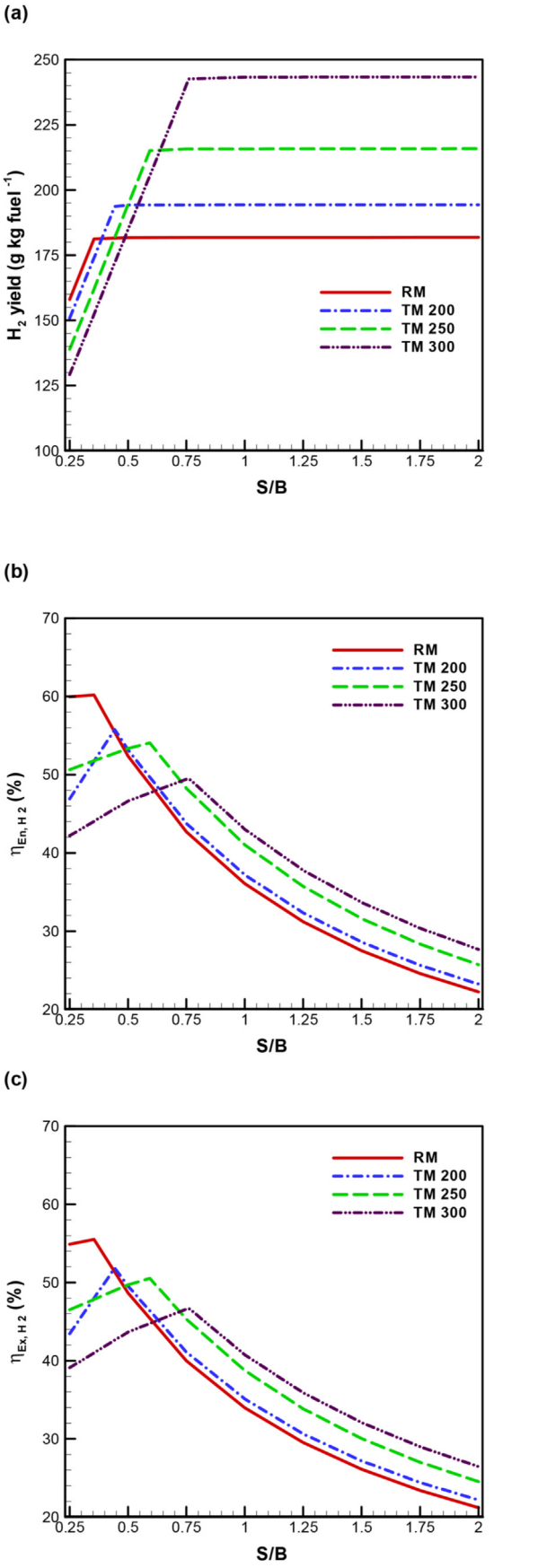

Fig. 7. Effect of the S/B ratio on the (a) hydrogen yield, (b) hydrogen thermal energy efficiency, and (c) hydrogen thermal exergy efficiency of four microalgal biomass fuels.

condition of CBP. Through a sensitivity analysis, it is found that the minimum amount of steam required to achieve the CO conversion of at least 85% in the HT-WGS reactor is 257 kg h^{-1} for RM, 288 kg h^{-1} for TM200, 319 kg h^{-1} for TM250, and 357 kg h^{-1} for TM300, corresponding to the inlet steam/CO molar ratio of approximately 4.07, 4.07, 4.09, and 4.13, respectively. Obviously, the higher the torrefaction temperature, the higher the amount of steam required, as a result of the enhancement of CO formation in the plasma gasifier after torrefaction.

Fig. 7a displays the distribution of hydrogen yield from the overall system for the four microalgal biomass materials as a function of S/B ratio. It can be observed that the hydrogen yield from the PSA outlet stream (S34) first increases noticeably with the S/B ratio and then becomes insensitive to it. From the sensitivity analysis, the optimal values of the S/B ratio for hydrogen production are also found to occur at the CBPs, where the hydrogen yields are 181.23 g kg-fuel^{-1}, 193.70 g kg-fuel^{-1}, 215.16 g kg-fuel^{-1}, 242.59 g kg-fuel^{-1}, respectively. The hydrogen yield enhancement is by 6.88%, 18.72%, and 33.86% when microalgae are torrefied at 200 °C, 250 °C and 300 °C, respectively. Fig. 7b and c shows the profiles of hydrogen thermal energy (η_{En,H_2}) and exergy (η_{Ex,H_2}) efficiencies as a function of S/B ratio. Similar to the curves of plasma energy ($\eta_{En,PG}$) and exergy ($\eta_{Ex,PG}$) efficiencies in Fig. 4c and d, the profiles of η_{En,H_2} and η_{Ex,H_2} of the four microalgal fuels are characterized by a maximum distribution. This can be attributed to the almost constant hydrogen yield after the CBPs, resulting in a significant decrease in η_{En,H_2} and η_{Ex,H_2}. Under the condition of CBPs, the optimum values of hydrogen thermal energy and exergy efficiencies (η_{En,H_2}, η_{Ex,H_2}) of RM, TM200, TM250, and TM300 are (60.17%, 55.49%), (55.77%, 51.85%), (54.05%, 50.53%), and (49.50%, 46.69%) respectively. From the viewpoint of hydrogen production, RM300 is the most appropriate fuel offering the highest hydrogen yield, but the hydrogen thermal energy and exergy efficiencies are reduced by 10.67% and 8.80%, respectively.

4.5. Life cycle assessment

The environmental impact of microalgae-based hydrogen process under the condition of CBPs are shown in Fig. 8. Fig. 8a displays a comparative life cycle GHG assessment of four different microalgal biomass materials to produce 1 kg of hydrogen and a breakdown of life cycle GHG emissions contributed by each unit. It is indicated that the largest contribution of life cycle GHG emissions is indirect GHG emissions associated with the drying of wet microalgae, followed by the steam plasma gasification of microalgae. Both energy-intensive processes account for 74.69%, 70.33%, 71.40%, and 71.25% of the total life cycle GHG emissions, corresponding to RM, TM200, TM250, and TM300, respectively. The third-largest contribution of life cycle GHG emissions comes from cultivation and harvest of microalgae stage, while the contributions from H_2 purification unit and direct CO_2 emissions from the microalgae-based hydrogen plant are almost equal. The net life cycle GHG emissions of RM, TM200, TM250, and TM300 are 1.53, 8.23, 10.73, and 13.07 kg CO_{2eq} kg-H_2^{-1} respectively, revealing that the severe the torrefaction temperature the higher amount of CO_2 is emitted, even though the value of CO_2 fixation attained in case of TM300 is the highest. This arises from the fact that (1) on account of low solid mass yield at higher torrefaction temperatures, more wet microalgal biomass is required to be treated to obtain 1 kg of torrefied microalgae, implying that greater electricity demand during microalgal cultivation, harvest, and drying process is needed as compared to RM, and (2) much higher plasma energy consumption for steam plasma gasification process is required in order to optimize the hydrogen yield.

The life cycle net energy ratio (NER) of RM, TM200, TM250, and TM300 is 0.347, 0.305, 0.279, and 0.255, respectively, as shown in Fig. 8b. Basically, the electricity demand for microalgal drying and steam plasma gasification is responsible for the majority of energy input, contributing to 76.59, 76.12, 74.08, 73.12% of energy input, corresponding to RM, TM200, TM250, and TM300, respectively. In this LCA study, the energy requirements for each unit are assumed to be obtained from a fossil fuel source of energy. By virtue of a considerable amount of indirect CO_2 emissions induced by the electricity demand of microalgal pretreatment (around

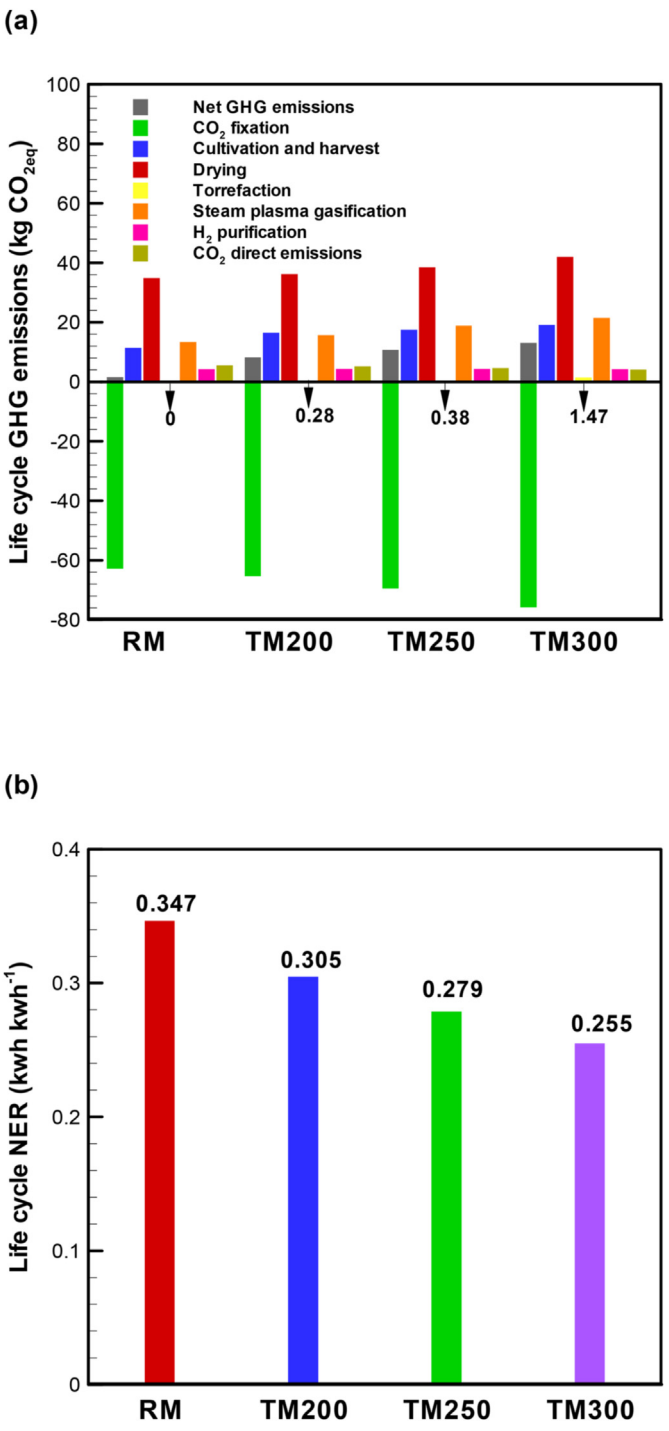

Fig. 8. Life cycle assessment of (a) GHG emissions and (b) net energy ratio of four microalgal biomass fuels.

12.55–22.27 kwh kg-H_2^{-1}) and steam plasma gasification (around 3.71–7.96 kwh kg-H_2^{-1}), it is very important to use alternative microalgal drying methods such as solar drying to reduce the indirect CO_2 emissions [48]. For the future work, as a result, integrating hybrid renewable energy systems (a combination of solar, wind, and geothermal energy sources) for low carbon electricity generation with the present system has to be carried out to further mitigate the environmental burdens and simultaneously improve the NER of the plasma-assisted hydrogen production plant from microalgal biomass.

5. Conclusions

In this work, 3E (energy, exergy, environmental) analyses of plasma-assisted hydrogen production process from microalgae are thermodynamically investigated. Four different microalgal biomass fuels (RM, TM200, TM250, TM300) have been comprehensively examined and compared in terms of various performance indicators by varying the S/B ratios. Based on the 3E analyses of the proposed system, the following conclusions are drawn:

1. Considering the syngas yield, hydrogen yield, $\eta_{En,PG}$, $\eta_{Ex,PG}$, η_{En,H_2} and η_{Ex,H_2}, the suggested operating conditions (S/B ratio) of RM, TM200, TM250 and TM300 are 0.354, 0.443, 0.593 and 0.760 respectively, which are also located at the CBPs. As a whole, under the condition of CBPs, the higher the torrefaction temperature, the better the syngas and hydrogen yields, but the lower the values of $\eta_{En,PG}$, $\eta_{Ex,PG}$, η_{En,H_2}, and η_{Ex,H_2}.
2. The syngas and hydrogen yields of microalgae can be significantly improved by a factor of 36.70% and 33.86% respectively, after experiencing torrefaction at 300 °C. It is thus concluded that torrefaction of microalgae is advantageous to syngas and hydrogen production, but the need for greater plasma energy lowers the overall system energy and exergy efficiencies.
3. The comparative LCA results show that the higher the torrefaction temperature, the higher the GHG emissions. This is on account of the greater electricity consumption related to the drying and plasma gasification of microalgae, resulting in a low value of NER.

Finally, from the environmental perspective, the supply of electricity from an appropriate location specific renewable energy systems could be a promising approach to further improve the present system performance. Moreover, from the economic aspect, a comprehensive techno-economic analysis of the proposed microalgae-based hydrogen production system using plasma technology requires further investigation in the future.

Credit author statement

Po-Chih Kuo: Conceptualization, Writing – review & editing, Biju Illathukandy: Conceptualization, Validation, Writing – review & editing. Wei Wu: Conceptualization, Resources, Writing – review & editing. Jo-Shu Chang: Conceptualization, Writing – review & editing.

Declaration of competing interest

The authors declare that they have no known competing financial interests or personal relationships that could have appeared to influence the work reported in this paper.

Acknowledgments

The authors would like to thank the Ministry of Science and Technology, Taiwan for the financial support of this research under the grant MOST 108-2917-I-564-039.

Abbreviations and Symbols

CBP	Carbon Boundary Point
E	energy (MW)
FT	Fischer-Tropsch
GHG	Greenhouse Gases
GWP	Global Warming Potential
HHV	Higher Heating Value (MJ kg^{-1})
HT	High Temperature
LCA	Life Cycle Analysis
LCI	Life Cycle Inventory
LCIA	Life Cycle Impact Assessment
LHV	Lower Heating Value (MJ kg^{-1})
LT	Low Temperature
MSW	Municipal Solid Waste
m	mass flow rate (kg s^{-1})
NER	Net Energy Ratio
P	pressure (atm)
PGE	Plasma Gasification Efficiency
PSA	Pressure Swing Adsorption
PSR	Plasma energy to Syngas production Ratio
RDF	Refuse-Derived Fuel
SOFC	Solid Oxide Fuel Cell
WGS	Water Gas Shift
$\dot{E}x$	exergy rates (MW)
h	specific enthalpy (kJ/kmol)
R	universal gas constant (kJ $kmol^{-1}$ K^{-1})
RM	Raw Microalgae
TM200	Torrefied Microalgae at 200 °C
TM250	Torrefied Microalgae at 250 °C
TM300	Torrefied Microalgae at 300 °C
$\dot{n}$	mole flow rate (kmol s^{-1})
s	specific entropy (kJ $kmol^{-1}$ K^{-1})
S/B	Steam-to-Biomass mass flow rate ratio
T	temperature (°C)
W	work (MW)
x	mole fraction

Greek letters

η	efficiency
β	correlation factor

Subscripts

0	standard reference state
En	energy
Ex	exergy
electric	electrical efficiency
eq	equivalent
PG	plasma gasification
plasma	plasma energy
PSA	pressure swing adsorption
torch	plasma torch
ch	chemical
ph	physical
i	species i

References

[1] Oruc O, Dincer I. Development and performance assessment power generating systems using clean hydrogen. Energy 2021;215:119100.
[2] Kuo PC, Chen JR, Wu W, Chang JS. Hydrogen production from biomass using iron-based chemical looping technology: validation, optimization, and efficiency. Chem Eng J 2018;337:405–15.

[3] Nami H, Ranjbar F, Yari M. Thermodynamic assessment of zero-emission power, hydrogen and methanol production using captured CO_2 from S-Graz oxy-fuel cycle and renewable hydrogen. Energy Convers Manag 2018;161:53–65.
[4] Lin KC, Lin YC, Hsiao YH. Microwave plasma studies of Spirulina algae pyrolysis with relevance to hydrogen production. Energy 2014;64:567–74.
[5] Nagarajan D, Lee DJ, Chang JS. Recent insights into consolidated bioprocessing for lignocellulosic biohydrogen production. Int J Hydrogen Energy 2019;44:14362–79.
[6] Meyer MA, Weiss A. Life cycle costs for the optimized production of hydrogen and biogas from microalgae. Energy 2014;78:84–93.
[7] Gutierrez Ortiz FJ, Serrera A, Galera S, Ollero P. Methanol synthesis from syngas obtained by supercritical water reforming of glycerol. Fuel 2013;105:739–51.
[8] Riboldi L, Bolland O. Comprehensive analysis on the performance of an IGCC plant with a PSA process integrated for CO_2 capture. Int. J. Greenh. Gas Con. 2015;43:57–69.
[9] Moneti M, Di Carlo A, Bocci E, Foscolo PU, Villarini M, Carlini M. Influence of the main gasifier parameters on a real system for hydrogen production from biomass. Int J Hydrogen Energy 2016;41:11965–73.
[10] Palma CF. Modelling of tar formation and evolution for biomass gasification: a review. Appl Energy 2013;111:129–41.
[11] Hlina M, Hrabovsky M, Kavka T, Konrad M. Production of high quality syngas from argon/water plasma gasification of biomass and waste. Waste Manag 2014;34:63–6.
[12] Munir MT, Mardon I, Al-Zuhair S, Shawabkeh A, Saqib NU. Plasma gasification of municipal solid waste for waste-to-value processing. Renew Sustain Energy Rev 2019;116:109461.
[13] PhG Rutberg, Bratsev AN, Kuznetsov VA, Popov VE, Ufimtsev AA, Shtengel SV. On efficiency of plasma gasification of wood residues. Biomass Bioenergy 2011;35:495–504.
[14] Diaz G, Sharma N, Leal-Quiros E, Munoz-Hernandez A. Enhanced hydrogen production using steam plasma processing of biomass: experimental apparatus and procedure. Int J Hydrogen Energy 2015;40:2091–8.
[15] Favas J, Monteiro E, Rouboa A. Hydrogen production using plasma gasification with steam injection. Int J Hydrogen Energy 2017;42:10997–1005.
[16] Adnan MA, Xiong Q, Hidayat A, Hossain MM. Gasification performance of *Spirulina* microalgae-A thermodynamic study with tar formation. Fuel 2019;241:372–81.
[17] Adnan MA, Xiong Q, Muraza O, Hossain MM. Gasification of wet microalgae to produce H_2-rich syngas and electricity: a thermodynamic study considering exergy analysis. Renew Energy 2020;147:2195–205.
[18] Duan PG, Yang SK, Xu YP, Wang F, Zhao D, Weng YJ, Shi XL. Integration of hydrothermal liquefaction and supercritical water gasification for improvement of energy recovery from algal biomass. Energy 2018;155:734–45.
[19] Lopez-Gonzalez D, Fernandez-Lopez M, Valverde JL, Sanchez-Silva L. Comparison of the steam gasification performance of three species of microalgae by thermogravimetric-mass spectrometric analysis. Fuel 2014;134:1–10.
[20] Duman G, Uddin MA, Yanik J. Hydrogen production from algal biomass via steam gasification. Bioresour Technol 2014;166:24–30.
[21] Chen WH, Kuo PC. Torrefaction and co-torrefaction characterization of hemicellulose, cellulose and lignin as well as torrefaction of some basic constituents in biomass. Energy 2011;36:803–11.
[22] Wu KT, Tsai CJ, Chen CS, Chen HW. The characteristics of torrefied microalgae. Appl Energy 2012;100:52–7.
[23] Lv X, Jiang Z, Li J, Wang Y, Tong D, Hu C. Low-temperature torrefaction of *Phyllostachys heterocycla cv. pubescens*: effect of two torrefaction procedures on the composition of bio-oil obtained. ACS Sustainable Chem Eng 2017;5:4869–78.
[24] Yu KL, Lau BF, Show PL, Ong HC, Ling TC, Chen WH, Ng EP, Chang JS. Recent developments on algal biochar production and characterization. Bioresour Technol 2017;246:2–11.
[25] Yang KC, Wu KY, Hsieh MH, Hsu HT, Chen CS, Chen HW. Co-gasification of woody biomass and microalgae in a fluidized bed. J Taiwan Inst Chem E 2013;44:1027–33.
[26] Guo P, Saw WL, van Eyk PJ, Stechel EB, de Nys R, Ashman PJ, Nathan GJ. Gasification reactivity and physicochemical properties of the chars from raw and torrefied wood, grape marc, and macroalgae. Energy Fuels 2017;31:2246–59.
[27] Kuo PC, Wu W, Chen WH. Gasification performances of raw and torrefied biomass in a downdraft fixed bed gasifier using thermodynamic analysis. Fuel 2014;117:1231–41.
[28] Janajreh I, Raza SS, Valmundsson AS. Plasma gasification process: modeling, simulation and comparison with conventional air gasification. Energy Convers Manag 2013;65:801–9.
[29] Minutillo M, Perna A, Bona DD. Modelling and performance analysis of an integrated plasma gasification combined cycle (IPGCC) power plant. Energy Convers Manag 2009;50:2837–42.
[30] Kuo PC, Illathukandy B, Wu W, Chang JS. Plasma gasification performances of various raw and torrefied biomass materials using different gasifying agents. Bioresour Technol 2020;314:123740.
[31] Carbo MC, Boon J, Jansen D, van Dijk HAJ, Dijkstra JW, van den Brink RW, Verkooijen AHM. Steam demand reduction of water-gas shift reaction in IGCC power plants with pre-combustion CO_2 capture. Int. J. Greenh. Gas Con. 2009;3:712–9.
[32] Hoya R, Fushimi C. Thermal efficiency of advanced integrated coal gasification combined cycle power generation systems with low-temperature gasifier, gas cleaning and CO_2 capturing units. Fuel Process Technol 2017;164:80–91.
[33] Oh SY, Yun S, Kim JK. Process integration and design for maximizing energy efficiency of a coalfired power plant integrated with amine-based CO_2 capture process. Appl Energy 2018;216:311–22.
[34] Prins MJ, Ptasinski KJ, Janssen FJJG. Thermodynamics of gas-char reactions: first and second law analysis. Chem Eng Sci 2003;58:1003–11.
[35] Kotas TJ. The exergy method of thermal plant analysis. Malabar (FL: Krieger Publishing Company; 1995.
[36] Ramachandran S, Yao Z, You S, Massier T, Stimming U, Wang CH. Life cycle assessment of a sewage sludge and woody biomass co-gasification system. Energy 2017;137:369–76.
[37] Guo F, Wang X, Yang X. Potential pyrolysis pathway assessment for microalgae-based aviation fuel based on energy conversion efficiency and life cycle. Energy Convers Manag 2017;132:272–80.
[38] Delrue F, Setier PA, Sahut C, Cournac L, Roubaud A, Peltier G, Froment AK. An economic, sustainability, and energetic model of biodiesel production from microalgae. Bioresour Technol 2012;111:191–200.
[39] Collet P, Hélias Arnaud A, Lardon L, Ras M, Goy RA, Steyer JP. Life-cycle assessment of microalgae culture coupled to biogas production. Bioresour Technol 2011;102:207–14.
[40] Campbell PK, Beer T, Batten D. Bioresource technology life cycle assessment of biodiesel production from microalgae in ponds. Bioresour Technol 2011;102:50–6.
[41] Papadaki S, Kyriakopoulou K, Tzovenis I, Krokida M. Environmental impact of phycocyanin recovery from Spirulina platensis cyanobacterium. Innov. Food Sci. Emerg. 2017;44:217–23.
[42] Dhanavath KN, Bankupalli S, Bhargava SK, Parthasarathy R. An experimental study to investigate the effect of torrefaction temperature on the kinetics of gas generation. J. Environ. Chem. Eng. 2018;6:3332–41.
[43] Kuo PC, Wu W. Thermodynamic analysis of a combined heat and power system with CO_2 utilization based on co-gasification of biomass and coal. Chem Eng Sci 2016;142:201–14.
[44] Pinto F, Gominho J, Andre RN, Gonçalves D, Miranda M, Varela F, Neves D, Santos J, Lourenço A, Pereira H. Improvement of gasification performance of Eucalyptus globulus stumps with torrefaction and densification pre-treatments. Fuel 2017;206:289–99.
[45] AlNouss A, McKay G, Al-Ansari T. Production of syngas via gasification using optimum blends of biomass. J Clean Prod 2020;242:118499.
[46] Huynh CV, Kong SC. Combustion and NOx emissions of biomass-derived syngas under various gasification conditions utilizing oxygen-enriched-air and steam. Fuel 2013;107:455–64.
[47] Aravind PV, Woudstra T, Woudstra N, Spliethoff H. Thermodynamic evaluation of small-scale systems with biomass gasifiers, solid oxide fuel cells with Ni/GDC anodes and gas turbines. J Power Sources 2009;190:461–75.
[48] Choi HI, Hwang SW, Sim SJ. Comprehensive approach to improving life-cycle CO_2 reduction efficiency of microalgal biorefineries: a review. Bioresour Technol 2019;291:121879.
[49] Adnan MA, Hossain MM. Gasification performance of various microalgae biomass-A thermodynamic study by considering tar formation using Aspen plus. Energy Convers Manag 2018;165:783–93.
[50] Ramirez AD, Rivela B, Boero A, Melendres AM. Lights and shadows of the environmental impacts of fossil-based electricity generation technologies: a contribution based on the Ecuadorian experience. Energy Pol 2019;125:467–77.